



A heat transfer model for high titania slag blocks

by H. Kotzé*, and P.C. Pistorius†

Synopsis

Titania slag is used as feedstock in the production of titanium dioxide pigment. It (titania slag) is the product of ilmenite smelting, a process whereby ilmenite is reduced at high temperature utilizing anthracite as a reducing agent. Although various slag tapping configurations are employed throughout the ilmenite smelting industry, the method of tapping the slag from the furnace into bell shaped cast steel pots, was the subject of investigation in this study.

The paper describes the formulation of a cooling model used to calculate and subsequently predict the temperature profile of a slag block during its cooling within the various cooling environments of pot cooling, air cooling and water cooling. The model was calibrated against actual internal slag temperature measurements and verified with information obtained from both pilot and industrial scale blocks. The paper concludes with solidification results and their practical implication.

Introduction

Titania slag—the primary product from ilmenite smelting— is tapped directly from the furnace into typically 20 tonne cast steel pots (moulds). Following several hours of cooling in these pots, the titania slag blocks are tipped out to continue cooling under water sprays, air or a combination of water and air. The storage area designated for the cooling slag blocks (known as the block yard) is a notoriously dangerous area due to as yet unexplained explosions of blocks which still have liquid cores. Knowledge of the solidification rate of a typical slag block, and understanding of the factors which determine solidification, can provide fundamental background information when conducting an investigation into such explosions and formulation of subsequent preventative actions.

This paper gives an overview of the assumptions, material properties and boundary conditions used in the construction of a heat transfer model for a typical titania slag block. Calibration of the model was conducted by fitting the internal slag block temperatures as predicted by the model, to actual internal

temperature measurements by adjusting the heat conduction value of the slag. Verification of the model is also discussed in brief. The paper concludes with an expression giving the thickness of the block shell as a function of time and a discussion of the parameters controlling the cooling rate.

Model formulation

The primary requirement from the block cooling model was that it should be able to calculate the temperature profile of a slag block as a function of time for a cooling cycle consisting of primary cooling within the slag pot (and ambient air), followed by water and/or air cooling of the standalone block. With the block mass as input parameter into the cooling model, it was capable of accommodating both the approximately 1.5 tonne blocks which were cast during the pilot plant campaigns, as well as the 18 tonne blocks typical of a large-scale ilmenite smelting operation. Additional input parameters included the tap temperature, slag chemistry (represented by the %FeO), and durations and sequence of the various cooling environments, i.e. pot cooling, air cooling and water cooling.

The following paragraphs describe the approach taken to construct the cooling model.

Simplifications

The pot shell is level with the upper surface of the block. This is a valid assumption when the pot is filled up to capacity. For smaller taps the pot edge will extend above the block surface providing a fin for heat transfer.

* Consensi Consulting CC, Mthunzini, South Africa.

† Carnegie Mellon University, Pittsburgh, USA.

The authors were with the Department of Materials Science and Metallurgical Engineering, University of Pretoria, when this research was performed.

© The Southern African Institute of Mining and Metallurgy, 2010. SA ISSN 0038-223X/3.00 + 0.00. This paper was first published at the SAIMM Conference, Heavy Minerals, 20-23 September 2009.

A heat transfer model for high titania slag blocks

The pot consists of a shell only, i.e. no provision is made in the cooling model for trunnions and feet. The additional mass and feet of the pot adds only slightly to the heat extraction capacity of the pot.

Given that conduction through the solidified solid slag shell is rate determining, the exclusion of the above detail will not alter the results of the slag block cooling results.

The slag density was assumed to be constant at 3.8 t/m³. Closer to the horizontal (flat) surface of the block the internal structure typically contains gas pores, which results in a less dense material when compared with the bulk of the block which has a solid appearance. This, combined with decrepitation occurring on the upper horizontal surface of the block during primary cooling, notably affects the accuracy of heat transfer predictions. However, in the absence of a detailed model of liquid flow and solidification shrinkage within the block during solidification, this effect was not taken into account.

The three-dimensional block was reduced to a two-dimensional wedge-shaped slice from the slag block, as depicted in Figure 1.

Energy balance

The primary partial differential equation to solve was (all symbols are defined at the end):

$$\rho_{slag} C_{pslag} \frac{dT}{dt} - k_{slag} \left(\frac{\partial^2 T}{\partial r^2} + \frac{\partial^2 T}{\partial z^2} \right) = 0 \quad [1]$$

A finite element model was constructed by Dr Johan Zietsman from Ex Mente* (a process modelling company) utilizing FlexPDE version 5.0.13, a fully integrated partial differentiation equation solver**. The full model specification and all the inputs (such as slag properties, calculation procedure for heat transfer coefficients and pot dimensions) were provided by the authors while Dr Zietsman performed the actual coding of the model within FlexPDE.

From the shape dimensional parameters provided as input, FlexPDE generates a mesh of triangular nodes (an example of which is given in Figure 2). With the allowable error set at 0.1%, FlexPDE adapted the mesh subsequent to consistency checks over the solutions of the partial differential equations. When required the node size and/or time step is reduced. A separate balance was performed to test that the overall energy balance closed.

To accommodate the change in the boundary conditions (from cooling of the combined slag block and pot system initially, to cooling of a slag block alone once the block is tipped out of the pot), two FlexPDE code files were constructed. The first file provided for a volume consisting of two materials (the block and pot) each with its own material properties. In this instance heat transfer from the pot and horizontal block surface to the surroundings was by natural air cooling. The second file was for the block on its own. Heat transfer to the surroundings could be selected as either natural air cooling or water cooling. Data transfer from the

first to the second file was established through the TRANSFER statement of FlexPDE. This statement enables full data sharing between different FlexPDE runs. The boundary conditions for both these stages are discussed later.

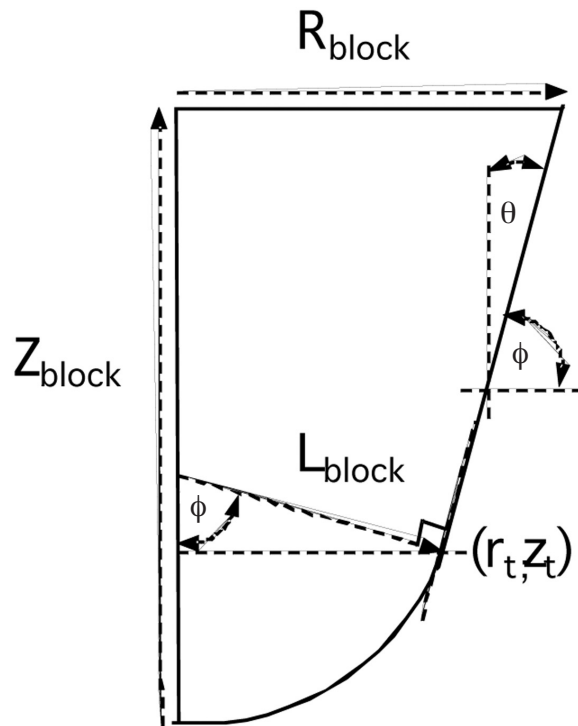


Figure 1—A two-dimensional slice from the block illustrating the important shape notations

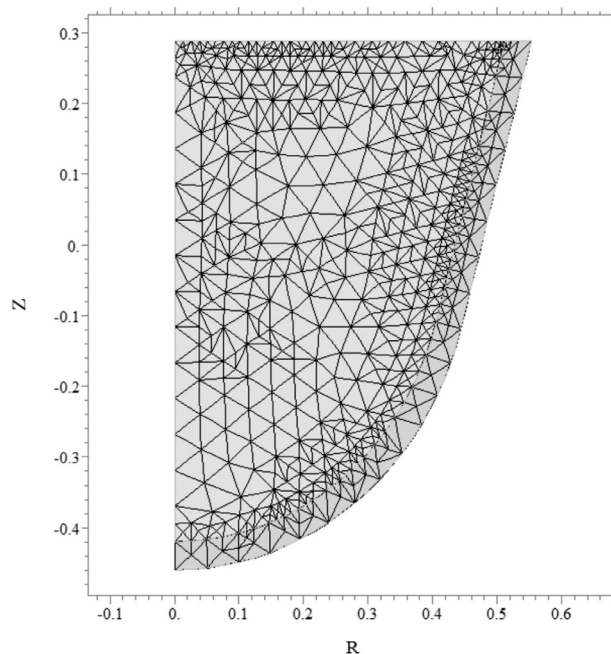
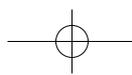


Figure 2—Example of the mesh configuration for the slag block (Z and R are in metres). Areas of denser node configurations are shown where FlexPDE reduced the node size to remain within the accuracy tolerance of 0.1%

*See www.ex-mente.co.za

**See www.pdesolutions.com



A heat transfer model for high titania slag blocks

Material properties

Slag thermodynamic properties

The liquidus and solidus temperatures of the slag, and the change in enthalpy of the slag with temperature, were estimated by means of FactSage¹, and approximated with simple mathematical relationships (based on the FeO content of the slag as the independent variable). The procedure followed is outlined below.

Choice of slag compositions

A database of 112 full plant slag analyses was obtained (elemental composition determined by X-ray fluorescence, and Ti³⁺ by titration) as are shown in Figure 3. The mass percentages of the other components varied approximately linearly with FeO content, for FeO levels ranging from just above 6% to more than 18%. These analyses were grouped together by FeO content, and an average analysis per FeO range was obtained (a valid approach, given the approximately linear variation of slag analysis with FeO content). These average analyses are listed in Table I. Note that these analyses are normalized to 100%; small amounts of other impurities (K₂O, V₂O₅, Nb₂O₅ and ZrO₂) making up less than 1% of the slag are hence neglected.

Thermodynamic properties

FactSage was used to predict the changes in phase

composition and enthalpy with temperature, for each of the eight slag compositions. The following phases (from the 'FT oxid' database of FactSage were considered):

- Solutions: SlagA, pseudobrookite (karrooite), Ca₃Ti₂O₇, Ca₃Ti₂O₆ and perovskite, and
- Stoichiometric solid phases: all relevant oxides, except the Ti_nO_{2n-1} Magnéli phases.

In addition to suppression of the Magnéli phases, ilmenite and spinel solid solutions were also not considered. This was done to ensure stability of pseudobrookite down to room temperature (which is in line with the observed persistence of pseudobrookite in the actual solidified slag).

Typical changes in the liquid fraction and enthalpy for one of the slags (no. 4 in Table I) are given in Figure 4. The continuous curves give the temperature dependence as predicted by FactSage. This shows a sharp decrease in liquid fraction just below the liquidus, with a tail extending to lower temperatures. For the purpose of the model, a linear approximation of this relationship was developed, matching the calculated profile at the liquidus temperature and at 20% solidification (indicated by T_{20} in the figure). The effective solidus temperature ($T_{solidus}$ in Figure 4) was found by extending the linear relationship to zero liquid.

A linear enthalpy relationship was similarly used as model input. This matched the calculated enthalpy at the liquidus temperatures, and in the fully liquid region (where FactSage reports a constant heat capacity). In the solid

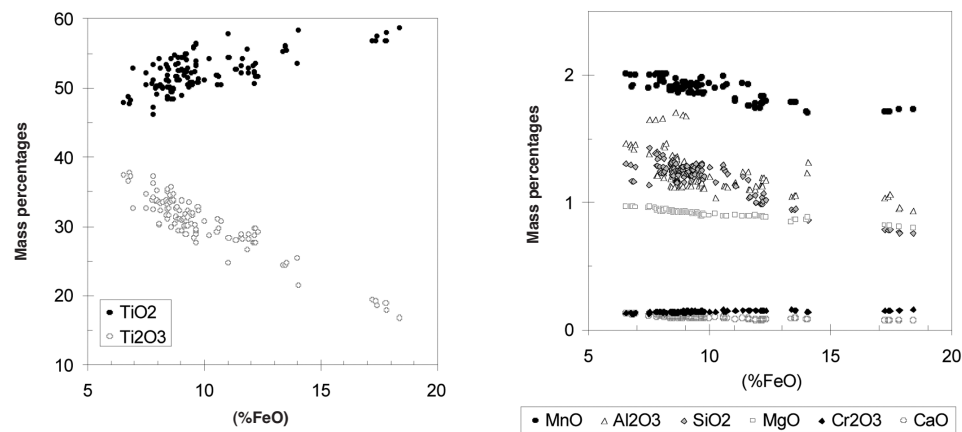
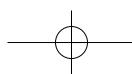


Figure 3—Analyses (mass%) of industrial plant slags

Table I

Average compositions (mass percentage) of eight groups of slags from the full plant data-set; each group spans a specific range of FeO contents

No.	FeO %	Ti ₂ O ₃ %	TiO ₂ %	MnO %	Al ₂ O ₃ %	SiO ₂ %	MgO %	Cr ₂ O ₃ %	CaO %
1	6.86	38.05	49.09	2.00	1.48	1.26	0.99	0.14	0.13
2	8.05	34.21	51.75	2.01	1.42	1.33	0.97	0.15	0.12
3	8.85	33.09	52.34	1.94	1.31	1.27	0.95	0.15	0.11
4	9.71	31.28	53.38	1.96	1.21	1.29	0.93	0.15	0.10
5	10.85	30.28	53.33	1.95	1.17	1.25	0.92	0.16	0.10
5	12.14	28.93	53.69	1.83	1.18	1.07	0.91	0.16	0.09
7	13.89	24.51	56.59	1.78	1.16	0.93	0.88	0.16	0.09
8	17.98	18.83	58.55	1.76	1.02	0.79	0.83	0.16	0.08



A heat transfer model for high titania slag blocks

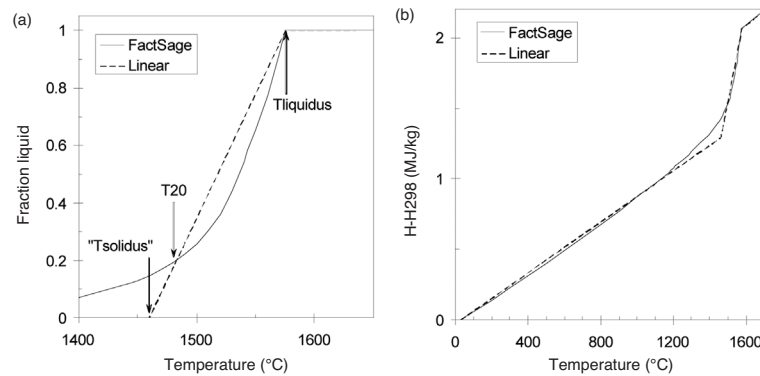


Figure 4—Predicted effect of temperature on (a) the fraction liquid and (b) the enthalpy (relative to that of solid slag at 298 K) of slag No. 4. The broken line gives the linear approximation which was used as model input

Table II

Parameters of linear approximations to thermodynamic properties, and fitted relationships

No.	%FeO	T_{liquidus} (°C)	' T_{solidus} ' (°C)	$C_{p\text{solid}}$ (J/kgK)	$C_{p\text{liquid}}$ (J/kgK)	H_{298}^{liquid} (MJ/kg)
1	6.86	1601.17	1470.34	903.60	1024.32	0.5014
2	8.05	1586.19	1451.36	903.73	1020.45	0.4989
3	8.85	1581.56	1463.56	902.75	1018.46	0.4957
4	9.71	1575.25	1459.53	901.88	1016.48	0.4916
5	10.85	1570.31	1453.99	900.64	1015.02	0.4867
6	12.14	1564.82	1450.26	898.56	1012.52	0.4819
7	13.89	1553.52	1440.63	896.46	1007.64	0.4745
8	17.98	1537.42	1427.74	891.26	1001.96	0.4510

region, the linear relationship matched the calculated trend at 298 K and at 1373 K (1373 K is just below the generally observed true solidus); all enthalpies were expressed relative to that of the solid at 298 K. The estimated solid enthalpy at the extrapolated solidus temperature, ' T_{solidus} ', was found by extrapolating this 298 K—1373 K linear relationship for the solidified slag; the enthalpy was also assumed to change linearly (between that of the solid slag and that of the liquid slag) over the temperature range ' T_{solidus} '— T_{liquidus} .

The linear approximations are given in Table II, while the fitted relationships are given in the following equations (all temperatures in °C, heat capacity in J/kg/K and enthalpy in J/kg):

$$T_{\text{liquidus}} = 0.2351(\%FeO)^2 - 11.24(\%FeO) + 1664.1 \quad [2]$$

$$T_{\text{solidus}} = 0.0364(\%FeO)^2 - 4.845(\%FeO) + 1502.7 \quad [3]$$

$$C_{p\text{solid}} = -0.0314(\%FeO)^2 - 0.4042(\%FeO) + 908.51 \quad [4]$$

$$C_{p\text{liquid}} = 0.0561(\%FeO)^2 - 3.3668(\%FeO) + 1044.4 \quad [5]$$

$$H_{298}^{\text{liquid}} = -139.51(\%FeO)^2 - 1086.1(\%FeO) + 515805 \quad [6]$$

$$f_{\text{liquid}} = \min\left(\max\left(\frac{T - T_{\text{solidus}}}{T_{\text{liquidus}} - T_{\text{solidus}}}, 0\right), 1\right) \quad [7]$$

The thermal conductivity of the slag was derived using actual slag internal temperatures as is discussed in the section on model calibration.

Pot thermodynamic properties

The heat capacity of the cast steel pot was assumed to be constant at 465 W/kg°C², while the thermal conductivity of the pot was expressed as a function of temperature as is shown in Equation [8]. Both these values are representative of a 0.5%C steel.

$$k_{\text{pot}} = -0.03488T + 59.1 \text{ W/m}^\circ\text{C}; T \text{ in } ^\circ\text{C} \quad [8]$$

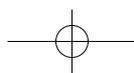
Boundary conditions

Contact resistances

Contact coefficient between the block and pot surfaces

A thermal contact resistance arises between the slag block and the pot, and this may affect the solidification process by lowering the rate of heat transfer from the block to the pot. In the case of titania slag cooling in a cast steel pot, the thermal contact resistance was found to be negligible: this is evident from the correspondence between the model predictions (which neglects contact resistance) and measured pot surface temperatures, shown in Figure 4(a). The locations of the dual thermocouples inserted into the pot shell are shown in Figure 9(b). If the contact resistance played a significant role, the actual pot temperatures would have been much lower than predicted; this is not the case.

Contact coefficient between the block and yard surface
During secondary cooling the horizontal surface of the block



A heat transfer model for high titania slag blocks

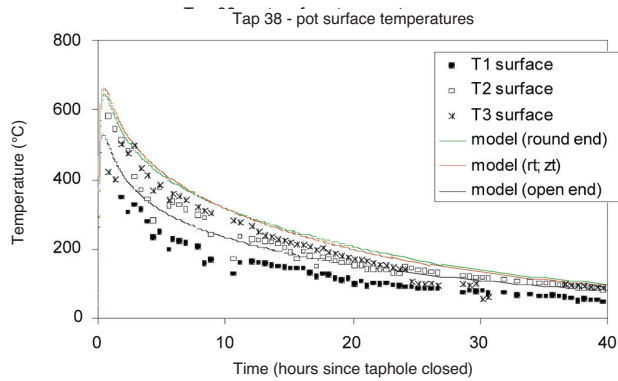


Figure 4(a)—Pot surface temperatures as predicted by the cooling model (lines). Symbols indicate surface measurements derived from actual temperature measurements within the pot shell

faces the block-yard surface. With the hot downward-facing surface effectively suppressing natural convection, this boundary condition was modelled via a contact resistance as per Equation [9], with k_{air} the thermal conductivity of air, d the average height of the air gap between the block and ground surfaces, and h_{rad} the radiation convection coefficient calculated as per Equation [10]. While the width of the gap between the block and yard surface varies, an average gap height of 10 mm was assumed. The model results were insensitive to the size of the air gap within a range of 5 mm to 50 mm.

$$h_{conduct} = \frac{k_{air}}{d} + h_{rad} \quad [9]$$

$$h_{rad} = \sigma \epsilon (T_{surface}^2 + T_w^2) (T_{surface} + T_w) \quad [10]$$

with temperature in K

Natural convection in air

During primary cooling in the pot, the pot outer surface and horizontal block surface are exposed to natural convection in

air. During this time the pot surface acts as an inclined heated surface facing downwards. After being tipped out of the pot, the conical and spherical surfaces of the block act as an inclined heated surface, facing upwards. The convection heat transfer coefficient for the above conditions was calculated from correlations and constants provided by Holman³ for natural convection in air. The joint effect of radiation and convection was expressed with an effective heat transfer coefficient. The resulting heat transfer coefficients for the horizontal and inclined surfaces are shown in Figure 5. At higher temperatures the contribution of radiation (bottom line in Figure 5) becomes increasingly predominant.

Forced spray water cooling

For the purposes of the block cooling model the heat transfer coefficient for spray water cooling was derived from the work of Klinzing *et al.*⁴, utilizing the original expressions of Mudawar⁵. Heat transfer coefficients calculated for varying volumetric flows, drop speeds and drop diameters are shown in Figure 6. Within the tested parameters range, the heat transfer coefficient is sensitive to the water volumetric flow rate, but insensitive to the drop diameter. Increasing drop speed moves the Leidenfrost temperature to higher values.

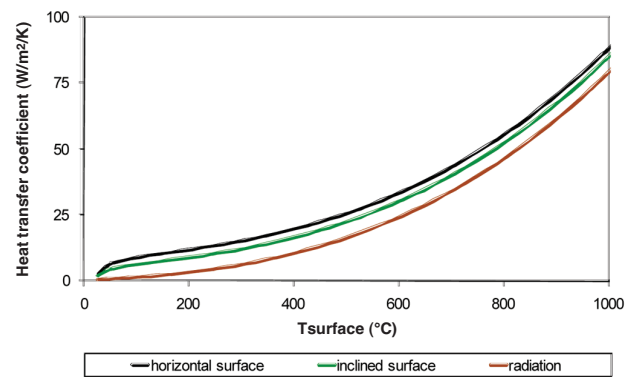


Figure 5—Heat transfer coefficients for natural cooling in air

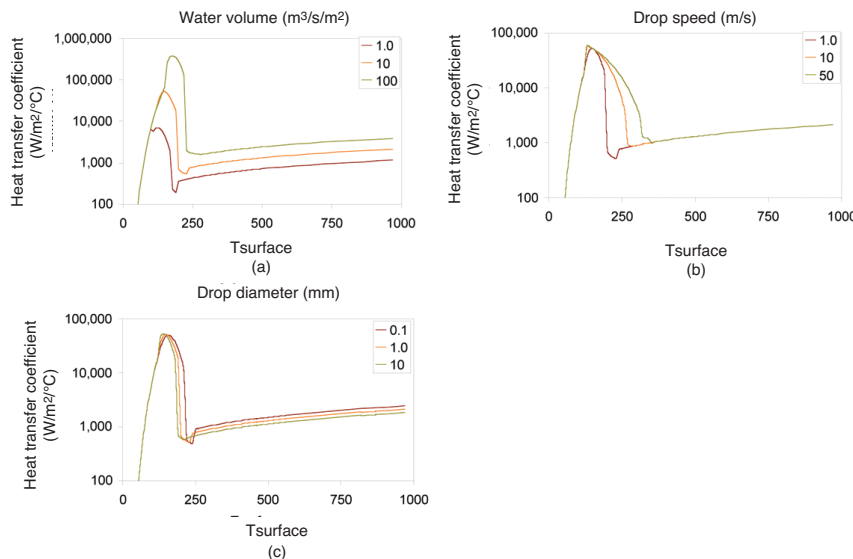
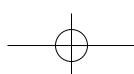
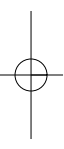


Figure 6—Heat transfer coefficients for cooling in water with varying (a) volumetric water flows (b) drop speeds and (c) drop diameters. Surface temperatures are in °C



A heat transfer model for high titania slag blocks

While the heat transfer coefficient in natural air cooling is usually around $10 \text{ W/m}^2\text{C}$, it increases by two to three orders of magnitude during spray water cooling.

Model calibration

During a pilot-plant ilmenite smelting campaign thermocouples were inserted into two slag blocks directly after tapping. These thermocouples were positioned as shown in Figure 7 and Figure 9. The configuration of the three centre line thermocouples is shown in Figure 8. The Alsint tube (alumina thermocouple sheath) was inserted into the silicon carbide tube and both these tubes were closed at the bottom end. Three 0.25 mm (wire diameter) type S thermocouple and sheath combinations were positioned within the Alsint tube at different heights as shown in Figure 9. The thermocouples marked A, B and C denote the thermocouples which were inserted down the centre line of the block; while those marked 1, 2 and 3 were double thermocouples inserted into holes drilled into the shell of the pot. The thermocouple inserted off centre into the block (Figure 7) failed and hence no data was obtained from it. The tap information and slag composition of the two taps are given in Table III and Table IV.

The thermal conductivity of titania slag is not a well known number—especially not as a function of temperature⁶. The model results were hence calibrated against the actual thermocouple measurements by adjusting the slag thermal

conductivity. The accuracy of the fit was determined by calculating the sum of the errors as per Equation [11]. The RMS error proved to be smallest with the thermal conductivity expressed as a linear function of temperature:



Figure 7—Photograph of a slag block and pot directly after thermocouples were inserted into the block. For support the refractory tubes were inserted into the slag through slots in a steel channel, which was placed horizontally over the pot edge

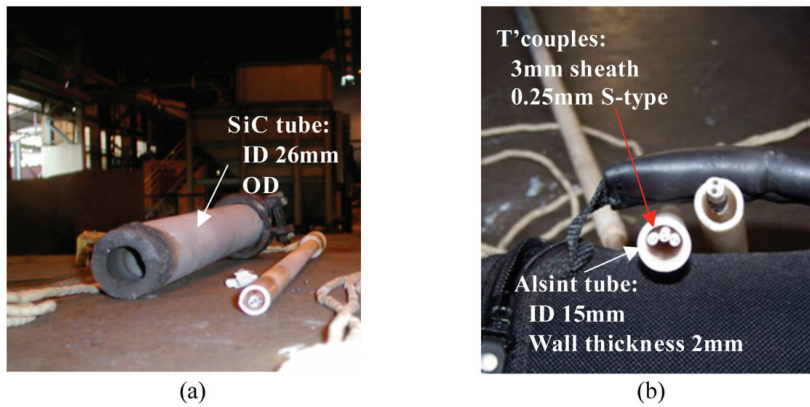


Figure 8—Photograph showing the configuration of the thermocouples which were inserted into the slag blocks

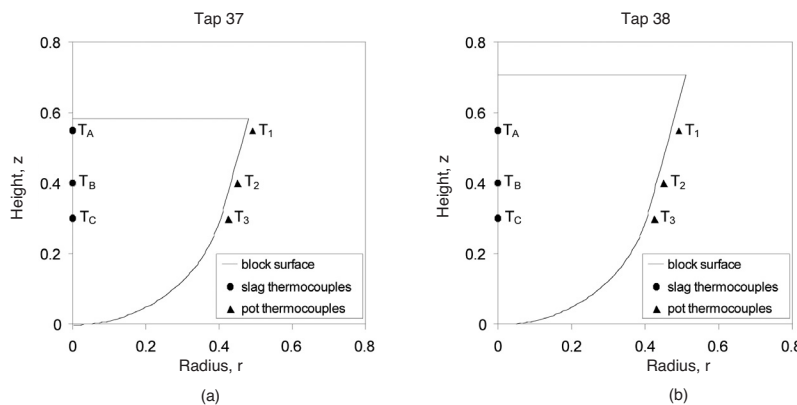
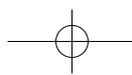


Figure 9—Thermocouple positions for blocks 37 and 38 tapped during Campaign 10. Alphabetic subscripts denote thermocouple positions inserted into the slag, while numeric subscripts denote positions of thermocouples inserted into the pot shell



A heat transfer model for high titania slag blocks

Table III
Tap chemistry (mass percentage) of the Campaign 10 pilot-plant blocks

	TiO ₂ %	FeO %	Al ₂ O ₃ %	CaO %	Cr ₂ O ₃ %	MgO %	MnO %	SiO ₂ %	V ₂ O ₅ %	Total %***
Tap 37	85.42	13.25	0.71	0.04	0.11	0.89	1.51	1.01	0.45	104.02
Tap 38	84.21	13.92	0.75	0.04	0.15	1.26	1.45	0.94	0.45	102.94

***The total exceeds 100% because Ti³ is usually reported as Ti⁴⁺ (TiO₂)

Table IV
Tap details of the Campaign 10 pilot-plant blocks

	Block mass (kg)	Tap rate (kg/min)	Tap temperature (°C)
Tap 37	1002	204.6	1669
Tap 38	1365	345.7	1668

$k = aT + b$. The best fit k value for each thermocouple is plotted in Figure 10. The uppermost thermocouple inserted into tap 37 (T_A) deviated substantially from the close grouping of the other five thermocouples. From visual observations, the upper layer of the slag block typically has a very porous structure. Hence, with thermocouple T_A being located high up in the block (Figure 9) it was likely positioned within this porous upper layer where the thermal conductivity is apparently dominated by the porous slag structure. The best fit k value for this layer seems to be constant at 0.5 W/m·°C, much lower than elsewhere in the block. As mentioned earlier, the effects of the porous structure of the upper layer were not included in the model; the thermal conductivity everywhere in the slag block was hence described by Equation [12].

$$RMS\ error = \sqrt{\frac{\sum (T_{actual}^i - T_{model}^i)^2}{n}} \quad [11]$$

$$k_{slag} = 0.00175T + 0.3\ W/m\cdot^{\circ}C; \quad [12]$$

The calibrated model results are compared with the actual internal temperature of the two pilot-plant slag blocks in

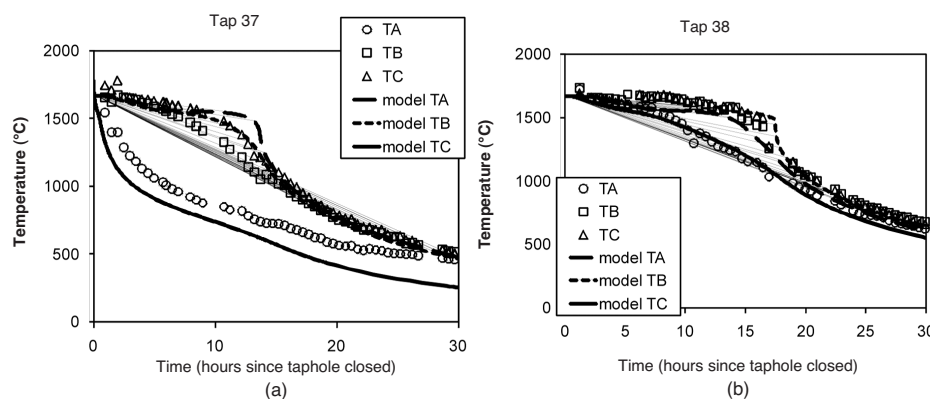


Figure 11—Internal slag temperatures for (a) tap 37 and (b) tap 38. Lines indicate model predictions, while symbols represent actual temperature measurements ($k = 0.00175T + 0.3$)

Figure 11. Apart from the cooling profile predicted for thermocouple T_A of tap 37 (for reasons as explained above), the model accurately predicts the actual measured temperatures. The fitted values of the thermal conductivity of the solidified slag—increasing from approximately 1 to 3 W/mK, for a temperature increase from 200°C to 1500°C—is in line with what is expected for this type of material, as discussed elsewhere.⁷

Model verification

The block cooling model was verified against the following information from 18 tonne (plant-scale) blocks: (i) the thickness of the crust after primary cooling (18 hours in the pot) and (ii) the surface temperatures of the block after 3 days of cooling under water sprays.

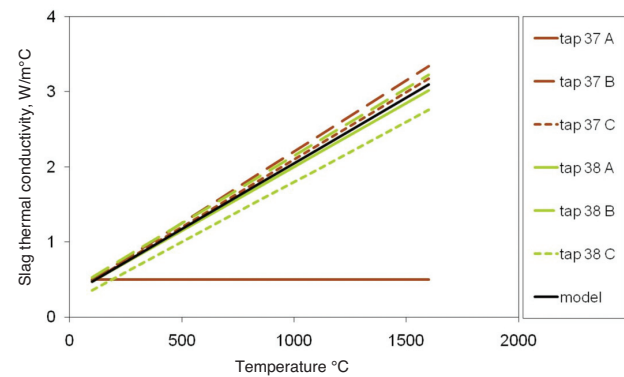
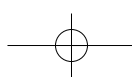


Figure 10—Best fit k values for taps 37 and 38. For modelling purposes the k value was expressed as given by the solid black line



A heat transfer model for high titania slag blocks

Crust thickness

In Figure 12 the thickness of the block shell after 18 hours of cooling in the pot shows clearly after the block disintegrated directly after being tipped out of the pot. In this instance the thickness of the shell is of the order of 300 mm to 320 mm. The model predicts the liquidus and solidus contours for a similar sized block cooled for an equal duration in the pot to be 371 mm and 276 mm from the round end of the block surface respectively (Figure 13). The actual crust thickness is therefore close to halfway between the liquidus and solidus contours. This fits in with observations and literature that the titania slags have a very high viscosity close to their melting point.

Surface temperatures

The surface temperatures of the two industrial-scale plant blocks were measured with an optical pyrometer when the spray water was stopped after 3 days. These temperatures are



Figure 12—Internal structure of a partially solidified block, as revealed by failure during tipping after primary cooling in the pot

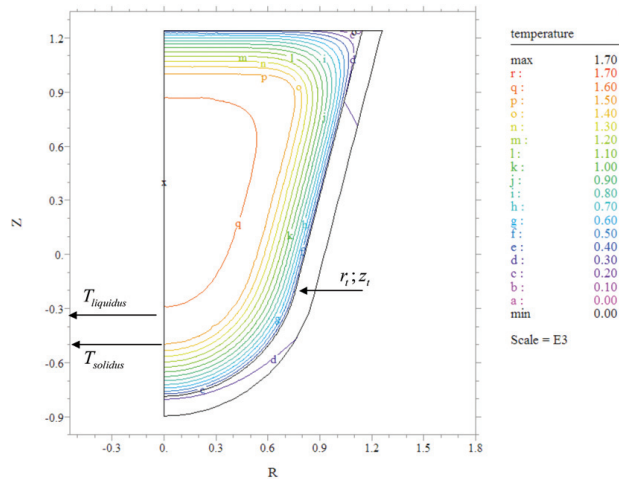


Figure 13—Temperature contours (scale in thousands of °C) of an 18 t block after 18 hours primary cooling (in pot)

shown in Figure 14 together with the model predicted surface temperatures of the block surface. The average surface temperature was calculated from two to four actual temperature measurements taken on the block surface. All temperatures were taken on the lower 0.5 m height band of the block. This band corresponds with the 0.6 m to 1.2 m marks on the Z axis (block height) of Figure 14 and Figure 15 (note that on the scales of these graphs Z=0 denotes the z_t height). The model predictions correlate well with the actual temperature measurements.

Solidification results

Following primary cooling the block is tilted out of the pot by means of an overhead crane. The block is then picked up by a front end loader and transported to the block yard. As soon as the front end loader is out of the range of the water sprays, the water is turned on. In view of this relatively crude handling method the thickness, strength and toughness of the crust at the end of primary cooling are important. Failure of the crust and subsequent trapping of water underneath liquid slag results in powerful hydrogen or steam explosions—an occurrence which must be avoided to prevent serious injury and/or damage.

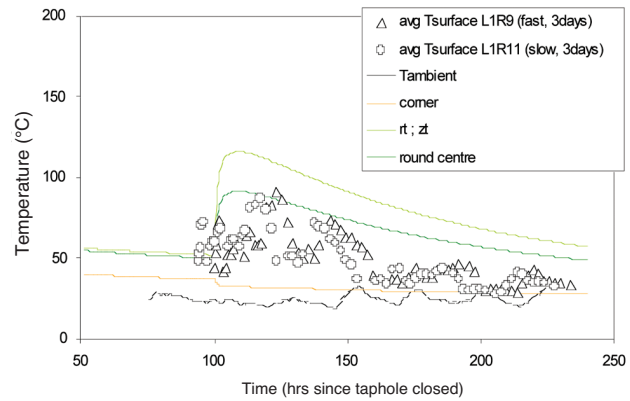


Figure 14—Surface temperatures of two 18-tonne blocks. Symbols represent actual measurements and lines represent model predictions

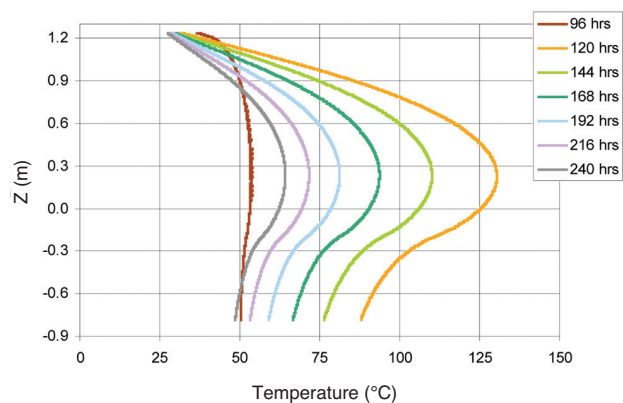


Figure 15—Surface temperatures of an 18-tonne block; times are expressed relative to the time of closing the taphole (the Z axis denotes height above ground level with the coordinate $(r_t; z_t)$ being at Z=0)

A heat transfer model for high titania slag blocks

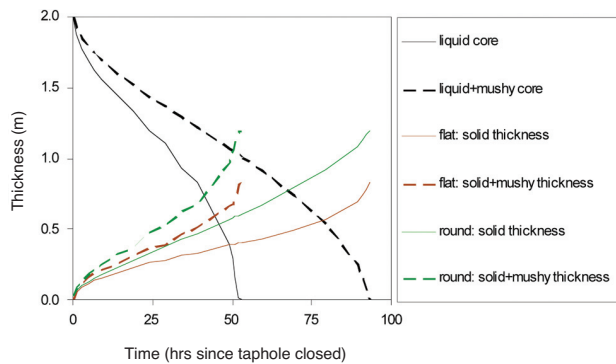


Figure 16—Remaining liquid core and shell thicknesses of a slag block cooling in a pot up to complete solidification

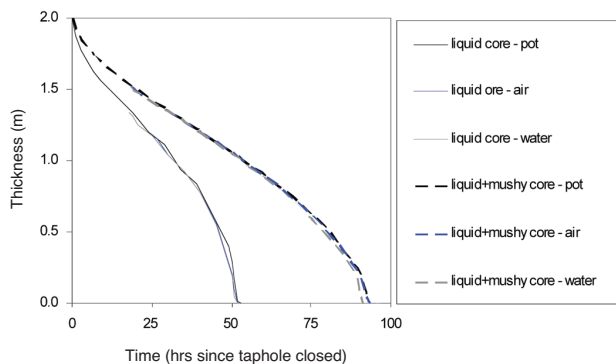


Figure 17—Comparison of the remaining liquid and mushy cores, for slag blocks cooled in the pot, in air and with water cooling

It is of interest to test whether this potentially unsafe situation can be eliminated by cooling the block in the pot for longer periods. In Figure 16 the growth of the shell along the vertical centre line of the block (z axis) for the flat and round ends of the block is shown. The last fully liquid node disappears between 52 and 53 hours of cooling. At this time the mushy zones (partially solidified slag, between liquidus and solidus temperatures), which are growing from the top and bottom, meet. The last mushy zones disappear between 92 and 93 hours. The solidification rates of a pot-cooled block are compared with those of water and air-cooled blocks in Figure 17: the water cooled block undergoes final solidification between 90 and 91 hours. Other than this relatively small difference in solidification time, the blocks solidify identically.

The shrinkage of the diameter of the liquid core along the block height (z axis) can be described by Equation [13]. Similarly the diameter of the mushy zone can be described by Equation [14]. In both instances d is in metres and t in hours, counting from the time of closing the taphole.

$$d_{\text{liquid}} = -2.413 \times 10^{-5} t^3 + 1.664 \times 10^{-3} t^2 - 5.696 \times 10^{-2} t + 1.951 \quad [13]$$

$$d_{\text{mushy}} = -2.041 \times 10^{-6} t^3 + 2.101 \times 10^{-4} t^2 - 2.135 \times 10^{-2} t + 1.847 \quad [14]$$

Discussion and conclusion

In the preceding paragraphs, the formulation of a cooling model for a titania slag block has been described. As part of this model formulation, useful material properties for titania slag (i.e. liquidus temperature, heat capacity numbers and enthalpy values) were described as functions of the slag chemistry as represented by the %FeO. Through calibration of the cooling model against actual internal slag temperature measurements, the thermal conductivity of titania slag as a function of temperature was also derived.

From the model predicted solidification results the following is concluded:

- The thermal conduction through the solid slag layer is the rate determining parameter of the cooling process. The practical implication is that the cooling method—whether pot, air or water cooling does not significantly alter the solidification rate of a slag block. The cooling environment does, however, substantially affect the surface temperature of the block.⁷
- An 18-tonne slag block is predicted to require just less than four days to solidify completely. Conservatively assuming the duration of primary cooling to be 20 hours, the shell thickness of the domed section of the block is predicted to be between approximately 270 mm and 370 mm. The thickness of the crust along the horizontal surface of the block can be expected to be even less if this region has a porous structure (a subsequence of the lower thermal conductivity at higher temperatures, Figure 10). This is an important point, in view of the fact that it is the horizontal surface which carries the load and handling during tipping at the end of primary cooling, and transport to the block yard.

Acknowledgements

The authors express their gratitude to the personnel from Exxaro KZN Sands and Exxaro R&D for their valued assistance during the campaign and pilot-plant research trials, as well as their permission to publish this work.

Nomenclature

- Z = maximum height of block (m)
 R = maximum radius of block (m)
 L = radius of block spherical section (m)
 θ = angle of block inclined surface with the vertical
 ϕ = angle of block inclined surface with the horizontal
 r_b, z_t = radius and height of the block where the conical and spherical sections meet
 V = volume (mp = area (m = density (kg/m^3))
 C_p = heat capacity (J/kgK)
 H = enthalpy (J/kg)
 k = thermal conductivity (W/mK)
 f = fraction
 T = temperature ($^{\circ}\text{C}$)
 h = heat transfer coefficient ($\text{W/m}^2\text{K}$)
 t = time (hours)
 d = distance or thickness (m)

A heat transfer model for high titania slag blocks

References

1. BALE, C.W., CHARTRAND, P., DEGTEROV, S.A., ERIKSSON, G., HACK, K., BEN MAHFOUD, R., MELANÇON, J., PELTON, A.D., and PETERSEN, S. FactSage Thermochemical Software and Databases. *Calphad*, vol. 26, 2002. pp. 189–228.
2. HOLMAN, J.P. *Heat Transfer*. McGraw Hill Book Co, SI Metric Edition, 1989. p. 635.
3. Holman, J.P. *Heat Transfer*. McGraw Hill Book Co, SI Metric Edition, 1989. pp. 331–345.
4. KLINZING, W.P., ROZZI, J.C., and MUDAWAR, I. Film and transition boiling correlations for quenching of hot surfaces with water sprays. *J. Heat Treating*, vol. 9, 1992. pp. 91–103.
5. MUDAWAR, I. and VALENTINE, W.S. Determination of the local quench curve for spray cooled metallic surfaces. *J. Heat Treat*, vol. 7, 1989. pp. 107–121.
6. TRAN, T., SOLNORDAL, C., and NEXHIP, C. Determination of thermal conductivity of titania slags. Unpublished CSIRO Minerals Report, DMR-2229, June 2003.
7. PISTORIUS, P.C. and KOTZÉ, H. The link between solidification of high-titania slag and subsequent comminution. Molten 2009, *Proceedings of the VIII International Conference on Molten Slags, Fluxes and Salts*, Santiago, Chile, January 2009; M. Sanchez, R. Parra, G. Riveros and C. Díaz (eds.). Gecamin, Santiago, Chile. 2009. pp. 51–60.
8. HANDFIELD, G. and CHARETTE, G.G. Viscosity and structure of industrial high TiO₂ slags. *Canadian Metallurgical Quarterly*, vol. 10, no. 3, 1971. pp. 235–243. ◆

From lead to gold, Air Liquide does it better



addictive AL1209/12449/2546

Air Liquide Southern Africa
Tel: +2711 389 7000, Kobus Durand (Metuallurgy Manager) +2711 389 7204
www.airliquide.co.za

Whether you are smelting lead or leaching gold, Air Liquide has the expertise, experience and gases to help you improve efficiencies, reduce costs and boost profits.

Our Pyretron burner system, for example, uses staged high-radiative technology to deliver a 50% higher melting rate, decreased energy cost, and other powerful advantages. Pyretron is popular with lead, aluminium, copper and brass smelters and for ladle preheating.

As for gold, ALDOC facilitates automatic control of the oxygen in cyanidation tanks, improving recoveries and decreasing costs. Talk to us about your processes and ask what we can do for you. Being the world's leader in industrial gases, we believe you'll like our answers.

ALDOC

There is an Air Liquide solution that's right for you.